ELSEVIER

Thermochimica Acta 392–393 (2002) 357–369

thermochimica acta

www.elsevier.com/locate/tca

Evaluation of kinetic parameters of thermal and oxidative decomposition of base oils by conventional, isothermal and modulated TGA, and pressure DSC

C.D. Gamlin[a], N.K. Dutta[a,*], N. Roy Choudhury[a], D. Kehoe[b], J. Matisons[a]

[a]*Ian Wark Research Institute, University of South Australia, Mawson Lakes, SA 5095, Australia*
[b]*Castrol Australia Pty. Ltd., Guildford, NSW 2161, Australia*

Abstract

Multigrade engine oils used in today's sophisticated engines are carefully engineered products. Different ingredients, such as viscosity index improvers, dispersants, antioxidants, detergents, antiwear agents, pour point depressants, etc. are added to the base oils to improve their performance as lubricants, significantly. However, the ultimate performance of the lubricant principally depends on the quality of the base oil. Therefore, understanding the degradation behaviour of the base oil is of significant importance. In this study, the kinetic parameters of the decomposition of different types and grades of base oils (all-natural, fully synthetic and semi-synthetic) have been investigated in detail by conventional and isothermal thermogravimetric analyses (TGA) as well as modulated TGA (MTGA®). Pressure DSC (PDSC) has been employed to evaluate the spontaneous ignition and oxidative degradation behaviour of the base oils. Base oils with higher viscosity within the same grade tend to degrade at higher temperatures. It appears that the degradation of the oils studied can be modelled by an *n*th-order mechanism and have similar activation energies of degradation under an inert atmosphere. The all-natural base oil ALOR100 is more resistant to oxidation than the semi-synthetic Yubase4 and fully synthetic PAO4 due to the presence of naturally occurring antioxidants.

Keywords: Base oil; Thermal decomposition; MTGA®; Pressure differential scanning calorimetry; Thermal analysis

1. Introduction

Formulation of an automotive lubricant is a complicated process. The modern engine lubricant is a carefully designed blend of base oils and performance enhancing additives, such as pour point depressants, antioxidants, dispersants and detergents [1,2]. Regardless of the complexity, the lubricant formulator must assess the performance of the base oil and additives, and finally balance performance to cost, before full-scale engine testing of the oil. Because engine testing is an expensive process, a number of bench tests have been developed to screen the lubricant throughout the formulation process [3]. Many of these bench tests are slow, man-power intensive, empirical, show poor reproducibility, and require a large investment in specialised equipment and skilled operators, and may be replaced, to advantage, by conventional thermal analysis techniques [4].

Carlson [5] has shown that volatility is the only parameter that can be directly linked to oil consumption. A number of efforts [6,7] have been made to simulate the Noack volatility test [8] using thermogravimetric

* Corresponding author. Tel.: +61-8-83023546.
E-mail address: naba.dutta@unisa.edu.au (N.K. Dutta).

0040-6031/02/$ – see front matter
PII: S0040-6031(02)00121-1

analysis (TGA). TGA has also been used to measure the volatility of additives as well as oils [9], and to measure oxidative volatility and deposit formation in oils [10]. Deposit formation has also been measured using pressure differential scanning calorimetry (PDSC) [11], and a correlation has been found between PDSC and the TFOUT method used to screen lubricants for the ASTM IIID and IIIE engine tests [9].

The useful life of the lubricating oil is determined by its oxidative stability, which is enhanced by hydrogenation of the base oil and addition of various oxidation inhibitors. However, the base oils are the major component of the lubricating oil, generally making up over 80% of the composition. Hence, the composition and properties of the base oil significantly affect the overall performance of the final lubricant [12]. Despite a number of papers exist on the crystallinity volatility and oxidative behaviour of formulated lubricating oils using normal technological and modern thermoanalytical techniques, there has been, to our knowledge, no work reported on the differences in volatility and oxidative behaviour of different classes of base oils.

Base oils may come from one of a variety of different sources, and the variations in composition directly affect lubricant performance. They can be roughly divided into three major classes of oil: all-natural; semi-synthetic; and fully synthetic. All-natural base oils are traditional petroleum oils made by the refinement of crude oil. During the refinement process, paraffinic waxes are typically removed from the oils, and these waxes can be hydrocracked to produce semi-synthetic oils. The fully synthetic oils are generally either long chain esters or low molecular weight poly-alpha-olefins (PAO).

In this study, we have investigated the effects of viscosity and base oil class on the thermal stability of base oils. The mechanism of base oil degradation in details has been examined using conventional, isothermal and modulated thermogravimetric techniques under an inert atmosphere. Pressurised DSC has been used to study the oxidative stability of the base oils.

2. Experimental

A series of fully synthetic (PAO), semi-synthetic (Yubase) and all-natural (ALOR) oil samples were received from Castrol Australia Pty. Ltd., and were used as received. The details of the oils used are shown in Table 1.

Table 1
Viscosities and oxidation onset temperatures for the oil samples studied[a]

Type	Sample grade	Viscosity (Pa s)	Oxidation onset temperature (°C)
Fully synthetic	PAO4	0.0350	202
	PAO5	0.0455	201
	PAO6	0.0595	197
	PAO7	0.0696	201
	PAO8	0.0870	197
Semi-synthetic	Yubase3	0.0252	198
	Yubase4	0.0301	198
	Yubase6	0.0695	200
All-natural	ALOR70	0.0211	213
	ALOR100	0.0402	248
	ALOR150	0.0554	252
	ALOR500	0.234	257

[a] Viscosities have been measured at shear rates of 100 s^{-1}, and oxidation onset temperatures taken from pressure DSC under 3.4 MPa oxygen at a heating-rate of 10 °C min^{-1}.

2.1. Rheology

Rheological characterisation was performed using a TA Instruments Rheolyst AR1000 controlled-stress rheometer fitted with a double concentric cylinder geometry to measure the viscosity of the samples. The samples were subjected to a continuous, logarithmic, controlled shear ramp from 0.1 to 5000 s^{-1} over a 5 min period at 25 °C. Viscosity was taken as the average of measurements over a 5 s interval at 100 s^{-1}.

2.2. Thermogravimetric analysis (TGA)

TGA analyses were conducted using a TA Instruments Hi-Res/Modulated TGA 2950 thermal analyser, using conventional (constant heating-rate), modulated and isothermal modes, operating from room temperature to 600 °C. The thermal analyser was temperature-calibrated between experimental methods using the Curie point of nickel as a reference.

2.2.1. Conventional TGA

Conventional TGA was performed on ~15 mg samples under a high-purity nitrogen atmosphere at

a flow rate of 50 ml min^{-1}. The samples were heated from ambient temperature to 500 °C at constant heating-rates of 2, 5 and 8 °C min^{-1}. The onset of degradation was taken as the temperature at which 5% decomposition occurred.

2.2.2. Isothermal TGA

Isothermal TGA of some representative samples were performed on ~15 mg samples under a high-purity nitrogen atmosphere at a flow rate of 50 ml min^{-1}. The samples were heated from ambient temperature to 250, 260 or 270 °C at a heating-rate of 20 °C min^{-1} before being held in isothermal mode until less than 1% of the sample remained.

2.2.3. Modulated TGA (MTGA®)

MTGA® of some representative samples was performed on ~15 mg samples under a high-purity nitrogen atmosphere at a flow rate of 50 ml min^{-1}. The samples were heated from ambient temperature to 400 °C at a heating-rate of 2 °C min^{-1}, with temperature amplitude of ±5 °C and a period of 200 s. The resulting TGA curve was analysed using TA Instruments' "Universal Analysis" program to obtain the activation energy of degradation across the entire weight loss for the samples.

2.3. Pressure differential scanning calorimetry (PDSC)

All PDSC was conducted using a TA Instruments DSC 2920 fitted with a constant-volume pressure cell, using conventional (constant heating-rate) and isothermal modes operating from room temperature to 300 °C. The DSC was calibrated between experimental methods using high-purity indium as a reference.

2.3.1. Constant heating-rate PDSC under oxygen atmosphere

Constant heating-rate PDSC was performed on ~5 mg samples in open aluminium pans under 3.4 MPa of high-purity oxygen. The samples were heated from ambient temperature to 300 °C at a constant heating-rate of 10 °C min^{-1}. The onset points of oxidation were calculated by extrapolation from the maximum heat flow to the extrapolation of the baseline.

2.3.2. Isothermal PDSC under oxygen atmosphere

Isothermal PDSC of some representative samples was performed on ~5 mg samples in open aluminium pans under 3.4 MPa of high-purity oxygen. Representative samples were heated from ambient temperature to the stated isothermal temperatures at a heating-rate of 50 °C min^{-1} before being held in isothermal mode until an exothermic peak of oxidation is measured.

3. Results and discussions

3.1. Rheology

Viscosity is by far the most significant property for establishing the thickness, pressure, and temperature of an oil film in hydrodynamic lubrication (HDL) and in elastohydrodynamic lubrication (EHL). Viscosity is an important factor in predicting the performance and fatigue life of rolling element bearing and gears. Viscosity is also used in equation for calculating the Summerfeld number, velocity in an oil film, fluid friction force, and power loss for hydrodynamic bearings. Lubricating oils have long chain hydrocarbon structures, and viscosity increases with chain length. The viscosities for all the oil samples were measured at shear rates ranging from 0.1 to 5000 s^{-1} at 25 °C. All samples showed Newtonian behaviour up to shear rates of 500 s^{-1}, and high-viscosity samples showed shear thinning at higher shear rates. The viscosities for the samples were taken as the average of measurements over a 5 s interval at a shear rate of 100 s^{-1}, and are shown in Table 1.

3.2. Thermogravimetric analysis (TGA)

3.2.1. Conventional TGA

Conventional TGA weight loss curves of the all-natural samples ALOR70, ALOR100, ALOR150 and ALOR500, performed at a constant heating-rate of 8 °C min^{-1}, are shown in Fig. 1. The decomposition of these samples occurs in a single step with no residue after the decomposition is completed. The broad temperature ranges over which the decompositions occur indicate that these samples have a broad molecular weight distribution. Similar behaviour has also been observed for Yubase and PAO4 series of oils.

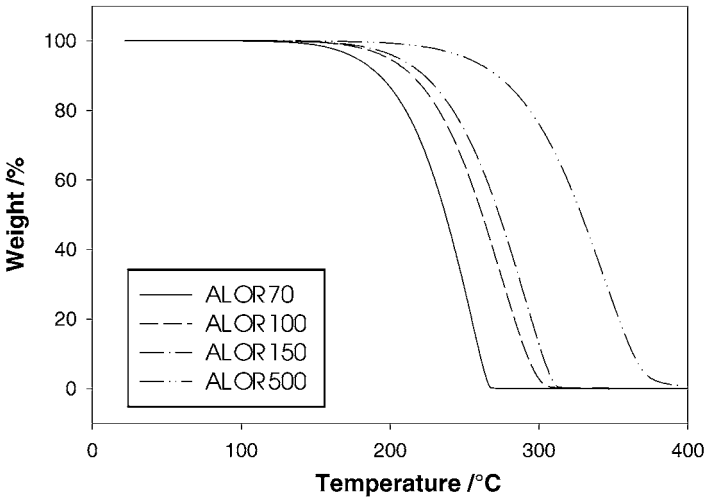

Fig. 1. TGA of ALOR series oils at a heating-rate of 8 °C min^{-1}.

Fig. 2 shows the relationship between sample viscosity and the onset and peak temperatures of degradation at 8 °C min^{-1} for all samples. It can be seen that the high-viscosity oil samples, such as ALOR500, degrade at higher temperatures than low-viscosity oil samples. This indicates that high-viscosity oil samples have higher thermal stability (lower volatility), and hence higher molecular weight, than low-viscosity oil samples. It is also worthwhile to note that the synthetic oils have higher thermal stability than the semi-synthetic and all-natural oils of similar viscosity, which may be due to a lower molecular weight distribution in the synthetic oils.

The kinetics of thermal transformation of a chemical reaction is generally described for a single step reaction by [13]

$$r = \frac{d\alpha}{dt} = k(T)f(\alpha) \quad (1)$$

where $f(\alpha)$ is the reaction model, α the extent of reaction, $k(T)$ the temperature dependent rate constant,

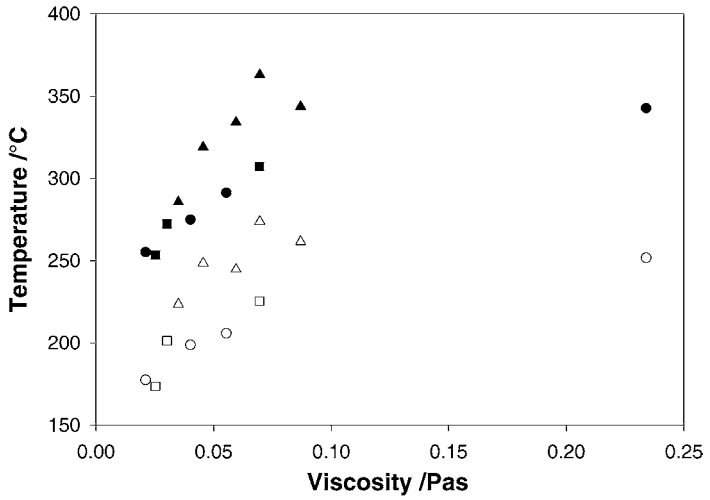

Fig. 2. Comparison between viscosity at 25 °C and onset and peak temperatures of degradation for the oil samples at a heating-rate of 8 °C min^{-1}. Circles are ALOR series, squares are Yubase series, and triangles are PAO series. Filled symbols are peak temperatures, and open symbols are onset temperatures.

'T' the temperature, 't' the time and 'r' the rate of degradation. The '$k(T)$' is normally assumed to obey the Arrhenius equation:

$$k(T) = A\exp\left(\frac{-E}{RT}\right) \tag{2}$$

where 'E' is the activation energy of the kinetic process, A the pre-exponential factor and R the universal gas constant.

The conversion dependent function, '$f(\alpha)$', is generally complicated and valid only for a limited range of experimental conditions. If it is assumed that the degradation reaction is a simple nth-order reaction, the conversion dependent term can be expressed as

$$f(\alpha) = (1-\alpha)^n = W^n \tag{3}$$

where, 'W' is the weight fraction remaining, and n the order of reaction.

Most published methods of deriving kinetic parameters from TGA are based upon these three equations. These methods involve analysis of either a single heating-rate thermogram, multiple thermograms with different heating-rates, isothermal thermograms, or thermograms obtained via dynamic or modulated heating-rates.

Integration of Eq. (1) yields:

$$F(\alpha) = \int_0^{\alpha}\frac{\mathrm{d}\alpha}{f(\alpha)} = k\int_0^{t}\mathrm{d}t \tag{4}$$

where the temperature increases with time at a constant heating-rate, ß $= \mathrm{d}T/\mathrm{d}t$, Eqs. (2) and (4) may be represented as

$$F(\alpha)\int_0^{\alpha}\frac{\mathrm{d}\alpha}{f(\alpha)} = \left(\frac{A}{\beta}\right)\int_0^{t}\exp\left(\frac{-E}{RT}\right)\mathrm{d}T \tag{5}$$

By using Doyle's approximation to the Arrhenius integral in Eq. (5), Flynn and Wall [14] and Ozawa [15,16] derived a method for the determination of activation energy based on:

$$\log\beta \cong -0.457\frac{E}{RT} + \left(\log\frac{AE}{RT} - \log F(\alpha) - 2.315\right) \tag{6}$$

Eq. (6) can be used to calculate the activation energy of degradation from multiple constant heating-rate data. If the mechanism of degradation is independent of the heating-rate, $F(\alpha)$ is constant for constant α, and the activation energy can be obtained from the slope of the straight-line by plotting $\log\beta$ versus $1/T$ for any level of conversion.

Conventional TGA has been performed on all samples at constant heating rates of 2, 5 and 8 °C min^{-1}. Fig. 3 shows a typical $\log\beta$ versus $-1000/RT$ plot constructed at 5, 10, 20, 30, 40, 50, 60, 70, 80 and 90% conversion. The parallel straight-line plots indicate there is little change in the activation energy of degradation throughout these degradation processes.

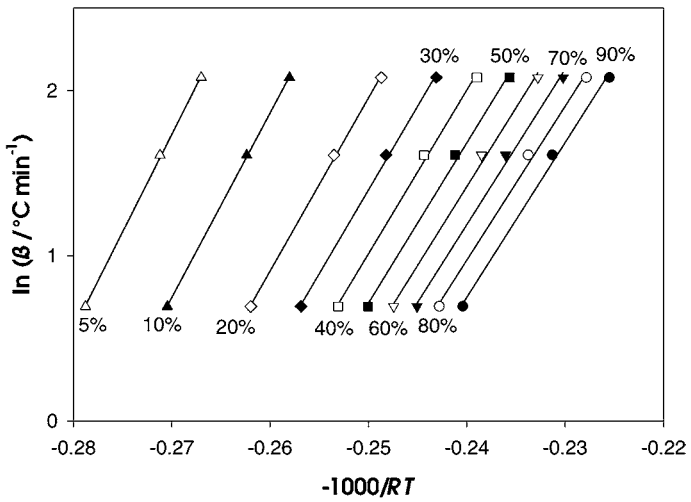

Fig. 3. Flynn–Wall–Ozawa plot for the degradation of ALOR70 at heating rates of 2, 5 and 8 °C min^{-1}.

Table 2
Activation energies of degradation calculated for all-natural oils using the Flynn–Wall–Ozawa method

Conversion (%)	Activation energy (kJ/mol)			
	ALOR70	ALOR100	ALOR150	ALOR500
5	108.7	79.60	97.48	93.38
10	103.1	77.68	100.5	93.52
20	94.61	78.29	99.08	96.21
30	89.98	79.03	95.55	98.64
40	86.86	79.59	93.64	100.6
50	84.30	79.84	92.50	102.0
60	82.02	79.84	91.64	103.1
70	80.42	79.38	90.90	104.5
80	79.71	78.62	90.35	105.8
90	80.62	78.44	90.23	107.8

Table 4
Activation energies of degradation calculated for fully synthetic oils using the Flynn–Wall–Ozawa method

Conversion (%)	Activation energy (kJ/mol)			
	PAO4	PAO6	PAO7	PAO8
5	100.6	91.65	80.97	86.00
10	97.97	87.84	80.15	93.52
20	97.18	86.86	78.91	100.4
30	97.53	89.51	78.65	104.1
40	97.82	93.02	78.96	107.2
50	98.05	95.25	80.19	110.6
60	98.03	95.69	82.48	114.7
70	97.82	95.30	84.59	120.3
80	97.96	96.00	86.22	127.9
90	103.1	100.4	88.57	132.3

The activation energies of degradation calculated at different conversion levels using the Flynn–Wall–Ozawa method for the all-natural, semi-synthetic and fully synthetic oils are shown in Tables 2–4, respectively. These tables clearly indicate that the activation energy of degradation is relatively constant throughout the degradation process for these oils. Although the oils studied are of different viscosities and from different oil classes, it can be seen that the activation energies of these oils are comparable.

Recently, Chan and Balke [17] proposed a method for calculating the activation energy of degradation of a sample from the thermogravimetric data of a single constant-heating-rate experiment. By assuming the reaction to be a first-order degradation, Eq. (7) can be derived as

$$\ln\left(\frac{r}{W}\right) = E\left(\frac{-1}{RT}\right) + \ln A \tag{7}$$

Therefore, for a first-order reaction, a plot of $\ln(r/W)$ versus $-1/RT$ should be a straight-line with slope equal to the activation energy.

These plots have been constructed for three samples of similar viscosity representing the three different classes of base oil studied: all-natural oil ALOR100, semi-synthetic Yubase4, and fully synthetic PAO4. A typical plot of $\ln(r/W)$ versus $-1000/RT$ for the samples studied is shown in Fig. 4. Although these plots deviate from the straight-line, at higher levels of decomposition, the oils behave as first-order decompositions up to at least 60% weight loss. Activation energies calculated for the linear regions of these plots from the data at three different heating-rates are shown in Table 5. The calculated activation energies at

Table 3
Activation energies of degradation calculated for semi-synthetic oils using the Flynn–Wall–Ozawa method

Conversion (%)	Activation energy (kJ/mol)		
	Yubase3	Yubase4	Yubase6
5	97.24	74.30	93.56
10	97.95	74.34	91.39
20	98.79	74.74	90.25
30	99.20	76.94	91.04
40	99.39	80.02	93.16
50	99.28	82.60	95.54
60	98.91	85.02	98.39
70	98.17	87.23	102.4
80	96.90	89.51	109.3
90	94.70	91.13	125.9

Table 5
Activation energies of degradation calculated using the method proposed by Chan and Balke for a representative set of oil samples

Heating-rate (°C min^{-1})	Activation energy (kJ/mol)		
	ALOR100	Yubase4	PAO4
2	86.80	85.66	105.47
5	83.37	84.33	101.73
8	82.76	84.39	93.99

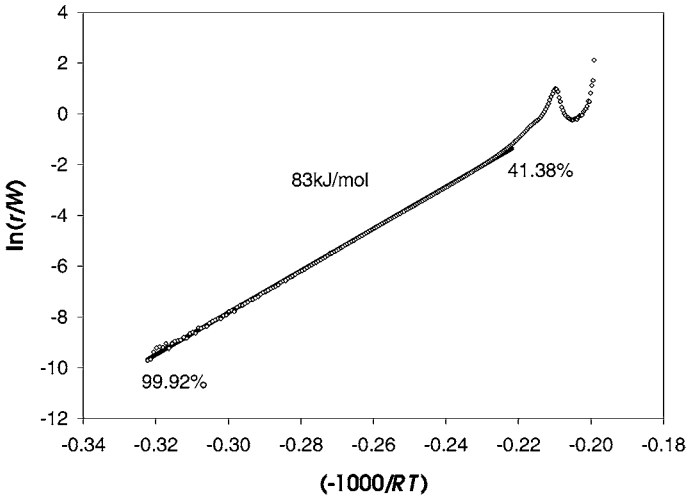

Fig. 4. A plot of the type proposed by Chan and Balke [17] for ALOR100 at a heating-rate of 8 °C min^{-1}. The weight remaining percentages over which a linear fit was obtained, as well as the activation energy calculated from that fit, are shown.

different heating-rates are within experimental error for each sample, and the synthetic oil has slightly higher activation energy of degradation than the semi-synthetic and all-natural oils.

3.2.2. Isothermal TGA

For a *n*th-order degradation at a constant temperature, we can derive Eq. (8) [18] as

$$\ln r = n \ln W + \ln k \tag{8}$$

Therefore, for an *n*th-order degradation, a plot of ln *r* versus ln *W* results in a straight-line with slope equal to *n*, and an intercept on the ln *r* axis of ln *k*. Using the natural logarithm of the Arrhenius Eq. (4), a further plot of $\ln k$ against $-1/RT$ provides the activation energy from the slope, and $\ln A$ from the intercept on the $\ln k$ axis (Eq. (9)).

$$\ln k(T) = E\left(\frac{-1}{RT}\right) + \ln A \tag{9}$$

Isothermal TGA was performed on ALOR100, Yubase4 and PAO4 at 250, 260 and 270 °C. Fig. 5 shows the temperature profile, weight loss and rate of degradation for ALOR100 at 270 °C, representative of the oil samples studied. For each sample up to 20% weight was lost while heating up to the desired isothermal temperature, and that the rate of degradation decays exponentially after the isothermal temperature is reached.

Fig. 6 shows that the plots of ln *r* versus ln *W* obtained from the isothermal data for ALOR100 and Yubase4 are straight line over the entire decomposition, indicating that these oils degrade via an *n*th-order mechanism. In comparison to these plots, PAO4 are slightly sigmoidal in nature, possibly indicating a change in mechanism over the course of the degradation. Nevertheless, straight-line fits to the PAO4 data have good correlation ($r^2 > 0.92$) and have therefore been treated as a single *n*th-order reaction. The Arrhenius plots for all three samples have good straight-line fits, giving activation energies of 74, 79 and 129 kJ/mol for ALOR100, Yubase4 and PAO4, respectively (Table 6).

The reaction-orders calculated from the Arrhenius plots for ALOR100 and Yubase4 change little with repect to temperature; average orders being 0.75 and

Table 6
Activation energies of degradation and orders of reaction calculated using the isothermal method for a representative set of oil samples

Temperature (°C)	Order of reaction *n*		
	ALOR100	Yubase4	PAO4
250	0.77	0.45	1.10
260	0.76	0.48	0.82
270	0.73	0.47	0.82
Activation energy (kJ/mol)	73.87	78.75	129.18

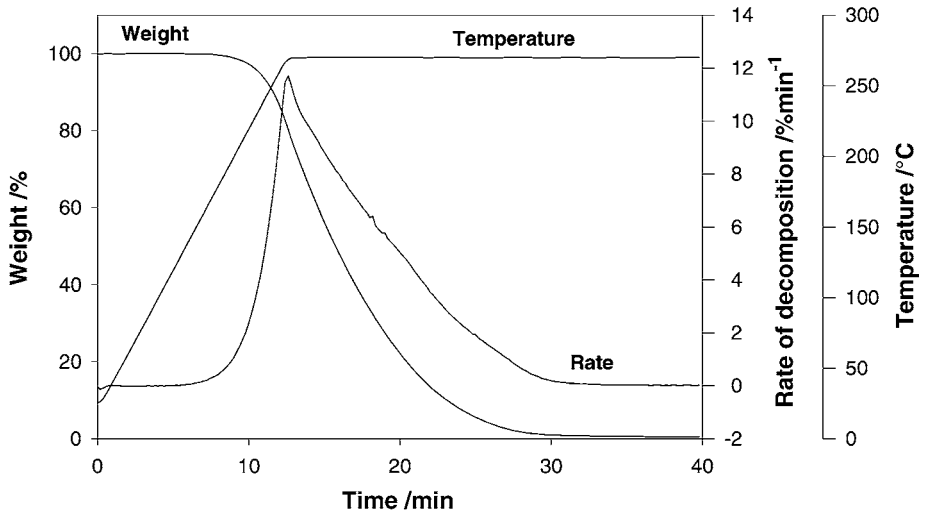

Fig. 5. Temperature profile, weight loss and rate of decomposition for the isothermal decomposition of ALOR100 at 270 °C.

0.47, respectively. However, the calculated order of reaction for PAO4 changes from 1.10 at 250 °C to 0.82 at 260 °C, again indicating a possible change in mechanism for the degradation reaction.

3.2.3. Modulated TGA (MTGA®)

Modulated TGA is based on a method first proposed by Flynn in 1968 [19]. It has recently been implemented [20,21] and patented by TA Instruments. In MTGA®, a sinusoidal temperature modulation is superimposed on the underlying linear heating-rate profile used in traditional TGA. These modulated-temperature results in an oscillatory response in the rate of weight loss (Fig. 7), deconvolution of which via real-time discrete Fourier transformation produces the desired kinetic parameters. The activation energy of

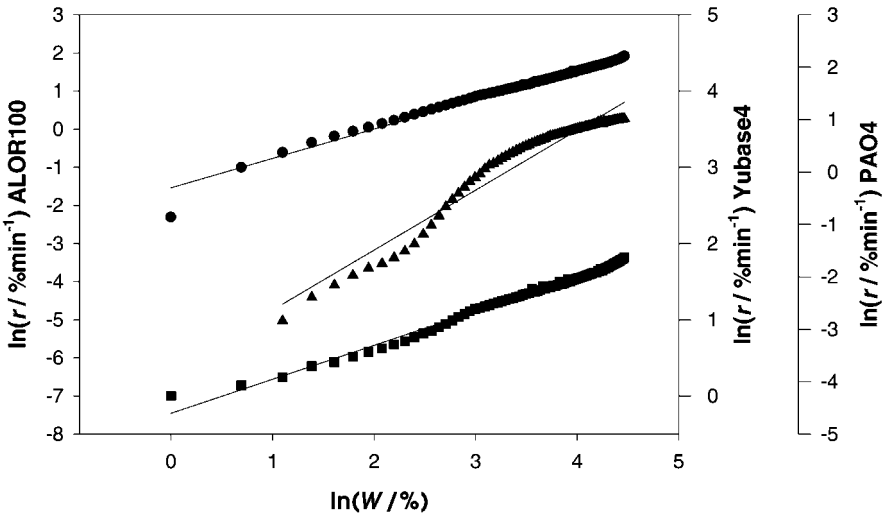

Fig. 6. Double log plots of degradation rate against fractional weight loss for ALOR100, Yubase4 and PAO4. Circles are ALOR100, squares are Yubase4, triangles are PAO4.

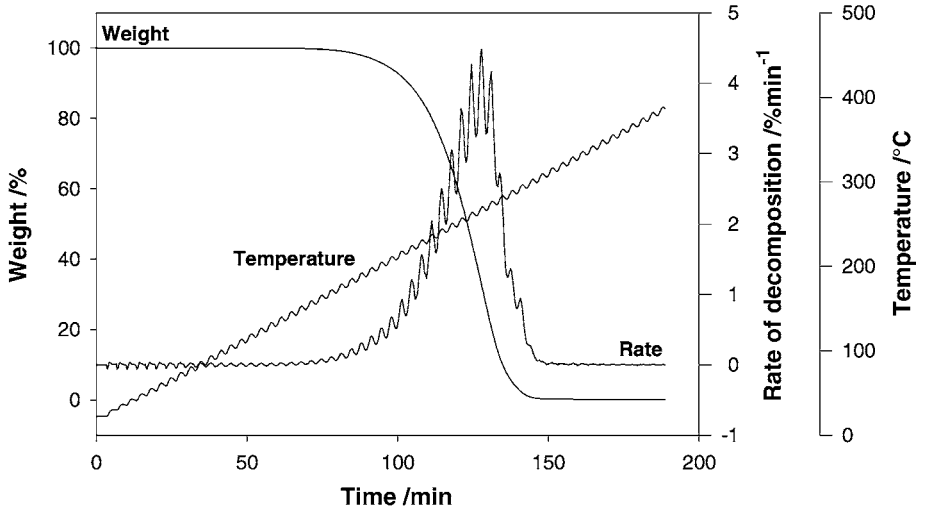

Fig. 7. Modulated-temperature program, showing the weight loss and the rate of decomposition for PAO4.

degradation can then be determined at any point in the decomposition reaction from Eq. (5):

$$E = \frac{R(T^2 - A^2)L}{2A} \tag{10}$$

where 'T' is the average temperature, A the temperature amplitude and 'L' the natural logarithmic ratio between the maximum and minimum rates of degradation as determined from the amplitude of the weight loss signal by discrete Fourier transformation [22].

Modulated TGA was performed on ALOR100, Yubase4 and PAO4, using an underlying heating-rate of 2 °C min^{-1}, with modulation amplitude of ±5 °C min^{-1} and period of 200 s. The activation energies calculated by MTGA® for these samples are relatively constant between 10 and 70% decomposition (Fig. 8). Over this range of decomposition, the average activation energies for ALOR100, Yubase4 and PAO4 are 95, 95 and 96 kJ/mol, respectively.

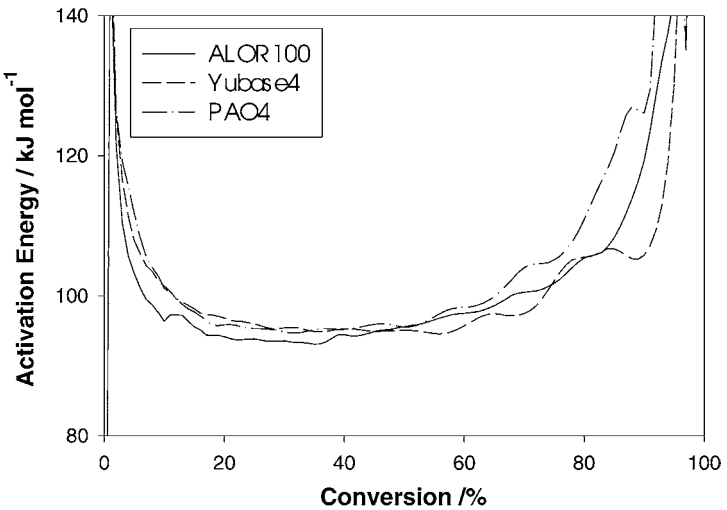

Fig. 8. Activation energies calculated as a function of conversion for ALOR100, Yubase4 and PAO4 using MTGA®.

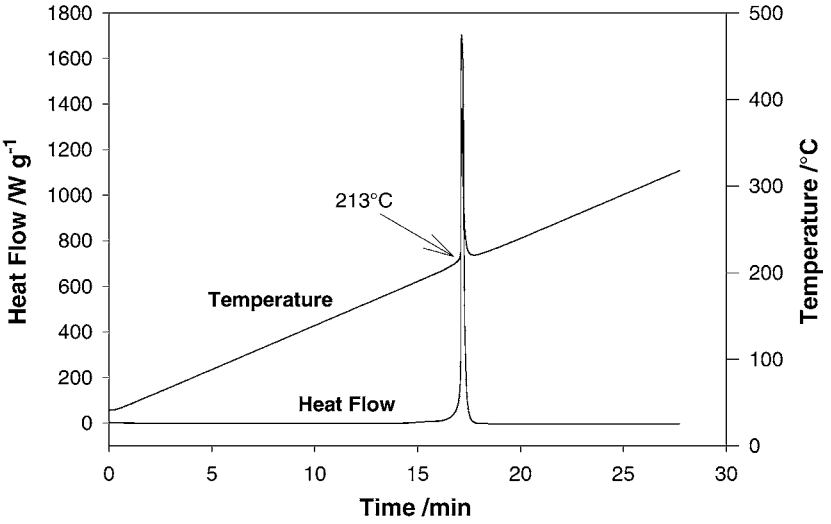

Fig. 9. Determination of the spontaneous ignition temperature of ALOR70.

3.3. Pressure differential scanning calorimetry (PDSC)

3.3.1. Constant heating-rate PDSC under oxygen atmosphere

Pressure DSC was used to determine the self-ignition temperatures for all the oil samples. Samples were heated at 10 °C min^{-1} to 300 °C under 3.4 MPa oxygen, and exhibited a sharp exotherm followed by rapid and complete decomposition of the sample (Fig. 9).

The all-natural oils generally underwent self-ignition at higher temperatures than the semi-synthetic and fully synthetic oils (Table 1). This may be due to the presence of naturally occurring nitrogen and sulphur containing species that act as antioxidants in the all-natural oils and are not present in the semi-synthetic and fully synthetic oils.

Basket et al. [23] used a similar method to determine the self-ignition temperature of fully-formulated ester-based aviation lubricants, and obtained temperatures of around 300 °C under air at 2 MPa and a heating-rate of 20 °C min^{-1}. The differences between the self-ignition temperature reported by Basket et al. and those reported in this paper may be due to the difference in the partial pressure of oxygen used in the test as much as the composition of the lubricant being tested.

3.3.2. Isothermal PDSC under oxygen atmosphere

The oxidative-induction time of the three representative oil samples was determined over a range of temperatures using pressure DSC. Oxidative-induction time [24] is a relative measure of the resistance of a material to oxidation, and can give valuable information regarding the performance of a material during both processing and service conditions.

Under 3.4 MPa high-purity oxygen, the samples were heated to a pre-determined temperature, before being held at this temperature until an exothermic peak of oxidation is measured. The oxidative-induction time is then taken as the time elapsed between reaching the pre-determined temperature, and the onset of oxidation, calculated by extrapolation from the maximum heat flow to the extrapolation of the baseline (Fig. 10). These oxidative-induction times are shown in Table 7.

It has been previously shown that oxidation occurs while heating to the isothermal test temperature, producing a bias in the measurement of the oxidative-induction time. This bias, which is usually less than 1.2 min [25,26], is small relative to the measured oxidative-induction times, and has therefore been ignored in this study.

For isothermal conditions, Eq. (4) may be restated as

$$F(\alpha) = A \exp\left(\frac{-E}{RT}\right) t \tag{11}$$

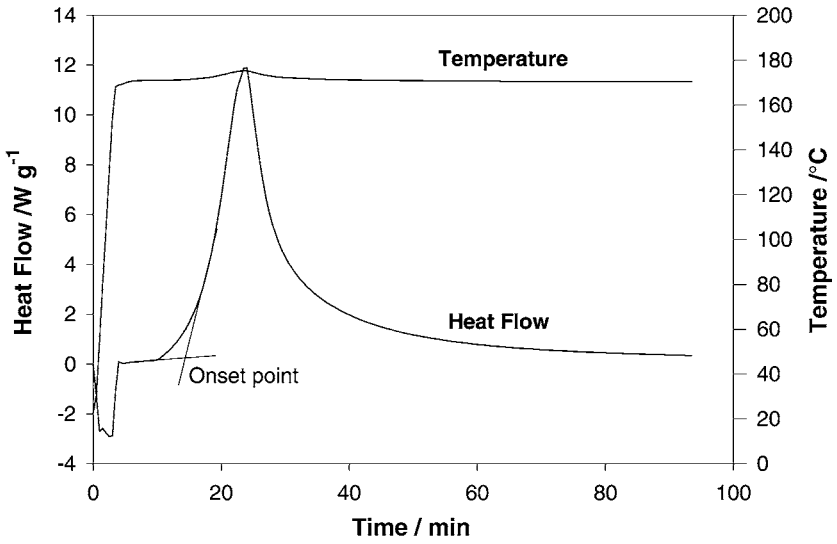

Fig. 10. PDSC thermogram and temperature profile for the oxidation of PAO4 with isothermal temperature set at 170 °C.

where t is the time to reach the level of conversion of interest.

Taking the logarithm of Eq. (11) and rearranging yields:

$$\ln t = E\left(\frac{1}{RT}\right) + \ln F(\alpha) - \ln A \qquad (12)$$

Therefore, if it is assumed that the onset or peak of the exotherm is reached at a constant level of conversion, independent of the reaction temperature, then the Arrhenius activation energy can be calculated using Eq. (12) [18]. The plot of time elapsed between reaching the isothermal temperature and either the onset or peak of the exotherm against $-1/RT$ should fall on a straight-line with slope equal to the activation energy. Eq. (12) may then be used to predict the oxidation induction time for the oil at any other temperature, assuming similar kinetics for decomposition.

Fig. 11 shows this type of plot for both the peak and onset of oxidation for ALOR100, Yubase4 and PAO4. Plots of this type show good correlation ($r^2 > 0.98$) for the samples studies, and the activation energies of the oxidative degradation process calculated for the representative oil samples using this method are shown in Table 8. These values are comparable to

Table 7
Oxidative-induction times of a representative set of oil samples under 3.4 Pa oxygen at a number of different isothermal temperatures

Sample	Temperature (°C)	Oxidative-induction time (min)
PAO4	140	117.29
	150	53.19
	160	21.88
	165	14.2
	170	13.18
Yubase4	140	66.06
	150	26.34
	160	13.24
	170	8.24
	180	5.21
ALOR100	180	124.39
	190	57.27
	200	25.59

Table 8
Activation energies of oxidative degradation calculated using 3.4 MPa oxygen under pressure DSC for a representative set of oil samples

Point of calculation	Activation energy (kJ/mol)		
	ALOR100	Yubase4	PAO4
Onset	141	98	118
Peak	199	133	130

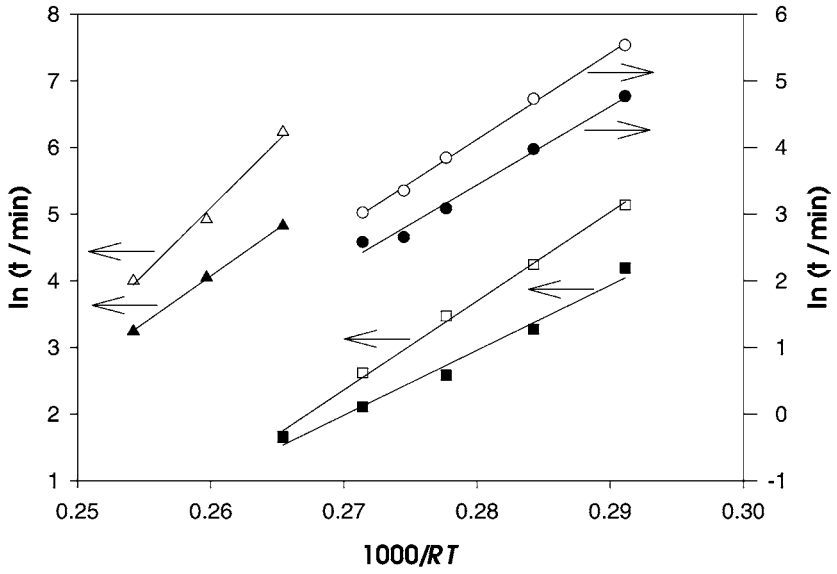

Fig. 11. Arrhenius plots for the onsets and peaks of the PDSC exotherms of ALOR100, Yubase4 and PAO4 at different isothermal temperatures. Triangles are ALOR100, squares are Yubase4, and circles are PAO4. Filled symbols are onset temperatures, and open symbols are peak temperatures.

the activation energy of 121 kJ mol^{-1} for a lubricating oil calculated by Walker and Tsang [27] using similar methodology.

It can be seen that the activation energy calculated from the peak of oxidation for the all-natural ALOR100 is significantly higher than those calculated for the semi-synthetic and fully synthetic base oils. This may be due to naturally occurring antioxidants in the all-natural base oil inhibiting the oxidation process.

4. Conclusions

The degradation of a range of base oils of different viscosities and oil types has been investigated by a variety of thermoanalytical techniques. Although oils with higher viscosity tend to degrade at higher temperatures, it appears that all the degradation of the oils studied can be modelled by a *n*th-order mechanism and have similar activation energies of degradation under an inert atmosphere. The all-natural base oil ALOR100 is more resistant to oxidation than the semi-synthetic Yubase4 and fully synthetic PAO4 due to naturally occurring antioxidants.

Acknowledgements

The authors are thankful to TA Instruments, especially to Roger Blaine, for helpful discussion, and Australian Research Council (ARC) for support of this work through collaborative grant scheme.

References

[1] R.M. Mortier, S.T. Orszulik (Eds.), Chemistry and Technology of Lubricants, VCH Publishers, New York, 1994.
[2] T.V. Liston, Lubr. Eng. 48 (1992) 389.
[3] A.E. Baker, in: E. Richard Booser (Ed.), Hand Book of Lubrication, Theory and Practice of Tribology, Vol. 1, CRC Press, Boca Raton, Florida, 1983, p. 481.
[4] R.L. Blaine, Am. Lab. 6 (1974) 18.
[5] D.C. Carlson, in: Proceedings of the SAE Intl. Congr. and Expo., Detroit, Michigan, 28 February–4 March 1983, p. 830029.
[6] M. Zinbo, L.M. Skewes, Thermochim. Acta 154 (1989) 367.
[7] B. Gustavsson, Thermochim. Acta 175 (1991) 73.
[8] DIN 51581 (1958).
[9] J.M. Perez, Thermochim. Acta 357 (2000) 47.
[10] H. Li, S.M. Hsu, Synth. Lubr. 13 (1996) 129.
[11] Y. Zhang, P. Pei, J.M. Perez, Lubr. Eng. 48 (1992) 189.
[12] D. Godfrey, W.R. Herguth, Lubr. Eng. 51 (1995) 397.

[13] M.E. Brown, D. Dollimer, A.K. Galway, Reaction in the Solid State: Comprehensive Chemical Kinetics, Elsevier, Amsterdam, 1980.
[14] J.H. Flynn, L.A. Wall, Polym. Lett. 4 (1966) 323.
[15] T. Ozawa, Bull. Chem. Soc., Jpn. 38 (1965) 1881.
[16] T. Ozawa, J. Therm. Anal. 2 (1970) 301.
[17] J.H. Chan, S.T. Balke, Polym. Degradation Stability 57 (1997) 135.
[18] M. Day, J.D. Cooney, D.M. Wiles, Polym. Eng. Sci. 29 (1989) 19.
[19] J.H. Flynn, in: R.F. Schwenker, P.D. Garn (Eds.), Thermal Analysis, Vol. 2, Academic Press, New York, 1969.
[20] R. Blaine, Am. Lab. 30 (1998) 21.
[21] R. Blaine, in: R. Morgan (Ed.), Proceedings of the Conference of the 24th North American Thermal Analytical Society, McLean, Virginia, 1997.
[22] R.L. Blaine, B.K. Hahn, J. Therm. Anal. Calorim. 54 (1998) 695.
[23] A. Basket, A. Zeman, K. Maier, Synth. Lubr. 15 (1968) 13.
[24] R. Boast, P. Latoszynski, Polymer 85 (1985) 165.
[25] S.M. Marcus, R.L. Blaine, ASTM Spec. Tech. Publ. STP1326 (1997) 172.
[26] R.L. Blaine, S.M. Marcus, J. Therm. Anal. 49 (1997) 1485.
[27] J.A. Walker, W. Tsang, Soc. Autom. Eng. Tech. Paper 801383, 1980.